Monte-Carlo Analysis of Asymmetry in Three-Site Relaxation Exchange: Probing Detailed Balance

Supplement

Bernhard Blümich,[1] Matthew Parziale,[2] and Matthew Augustine[2]

[1] Institut für Technische und Makromolekulare Chemie, RWTH Aachen University, Worringer Weg 2, 52074 Aachen, Germany: bluemich@itmc.rwth-aachen.de

[2] Department of Chemistry, UC Davis, One Shields Avenue, Davis, CA 95616, USA: mjparziale@ucdavis.edu, maugust@ucdavis.edu

Neighborhoods explored in 2D vacancy-diffusion simulations

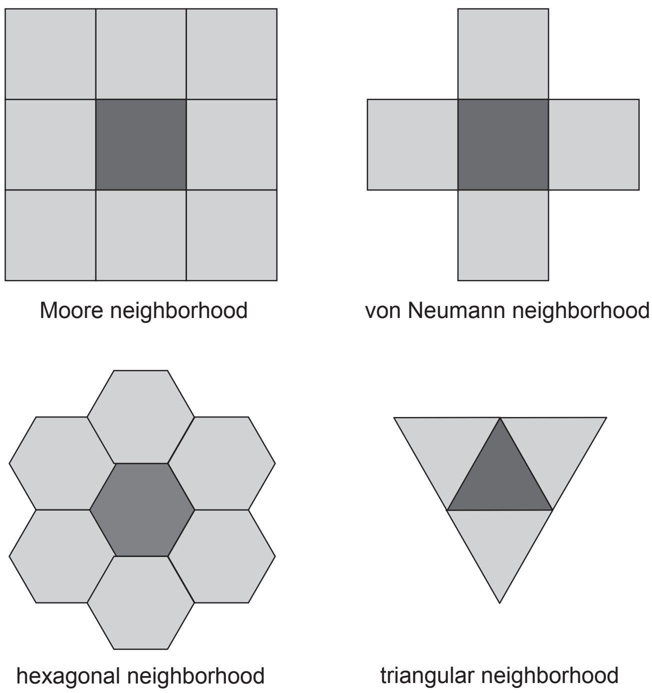

Figure S1. Simulation neighborhoods (grids) of range 1 for jumps from the center position (dark grey) to neighbor positions (light grey). All three asymmetry parameters from Eqn. (4) were calculated at each simulation run. Only the vacancy-diffusion simulations produced with the Moore neighborhood obeyed Eqn. (4), while all gas-diffusion simulations did.

Explicit example for the calculation of ΔU and ΔS of an initial configuration and 5 possible final configurations (cf. Fig. 2)

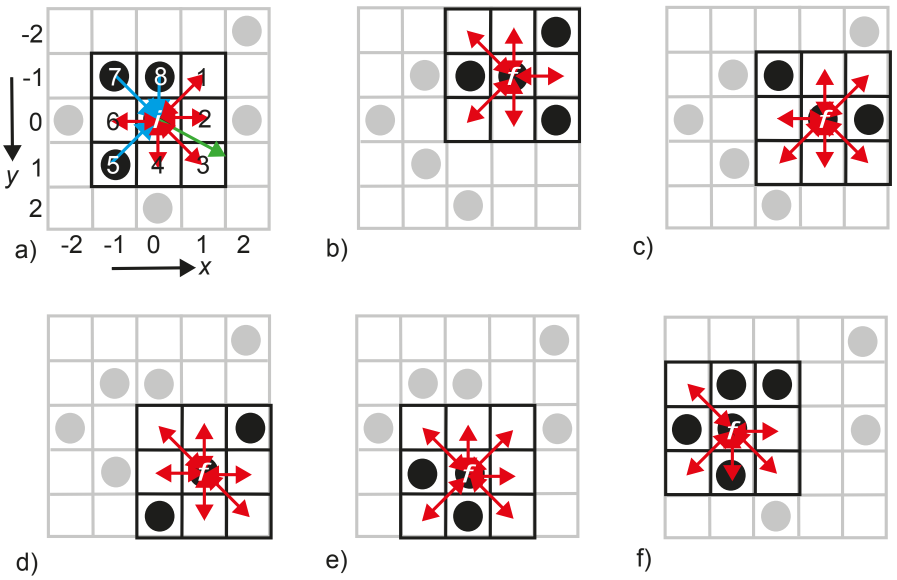

Figure S2 = Figure 2. Example for tic-tac-toe simulation of confined translational diffusion. a) Definition of coordinate frame. Cells with full circles are occupied. The initial particle position is marked by *i*, the final position by *f*. Forces, distances and entropies are estimated from the occupation of the 8 cells surrounding the cell of interest. The forces (blue arrows) on the particle occupying the initial position result from the sum (green arrow) of forces from the three occupied neighboring cells 3, 7, and 8. Entropy is estimated from the distances of the central particle to the neighboring empty cells (red arrows). b-f) Illustrations to estimate the entropies of the final configurations.

- Calculation of internal energy change $\Delta U = \boldsymbol{F}\,\Delta \boldsymbol{s}$:

$$\boldsymbol{F} = \left[0+0+0+0+\frac{1}{2^{3/2}}\begin{pmatrix}-1\\1\end{pmatrix}+0+\frac{1}{2^{3/2}}\begin{pmatrix}-1\\-1\end{pmatrix}+\begin{pmatrix}0\\-1\end{pmatrix}\right]=\begin{pmatrix}-2^{-1/2}\\-1\end{pmatrix},$$

$$\Delta\boldsymbol{R}_1=\begin{pmatrix}1\\-1\end{pmatrix},\Delta\boldsymbol{R}_2=\begin{pmatrix}1\\0\end{pmatrix},\Delta\boldsymbol{R}_3=\begin{pmatrix}1\\1\end{pmatrix},\Delta\boldsymbol{R}_4=\begin{pmatrix}0\\1\end{pmatrix},$$

$$\Delta\boldsymbol{R}_5=\begin{pmatrix}0\\0\end{pmatrix},\Delta\boldsymbol{R}_6=\begin{pmatrix}-1\\0\end{pmatrix},\Delta\boldsymbol{R}_7=\begin{pmatrix}0\\0\end{pmatrix},\Delta\boldsymbol{R}_8=\begin{pmatrix}0\\0\end{pmatrix}.$$

The values of $\Delta U = \boldsymbol{F}\Delta\boldsymbol{R}$ for the 8 neighboring cells are

$$\Delta U = \boldsymbol{F}\,\Delta\boldsymbol{R} = \left\{-2^{-\frac{1}{2}}+1, -2^{-\frac{1}{2}}, -2^{-\frac{1}{2}}-1, -1, 0, 2^{-\frac{1}{2}}, 0, 0\right\}.$$

- Note: A better approximation of the force would be to calculate the average force as $\boldsymbol{F} = (\boldsymbol{F}_f + \boldsymbol{F}_i)/2$.
- Estimation of entropies S from the distances $|\Delta\boldsymbol{R}|$ to all 8 neighbors in the particle-centered tic-tac-toe frame:

Initial state (Fig. 2a): $S_i = 2^{\frac{1}{2}}+1+2^{\frac{1}{2}}+1+0+1+0+0 = 3+2\,2^{\frac{1}{2}}$

Final state 1 (Fig. 2b): $S_f = 0 + 1 + 0 + 1 + 2^{\frac{1}{2}} + 0 + 2^{\frac{1}{2}} + 1 = 3 + 2\ 2^{\frac{1}{2}}$

Final state 2 (Fig. 2c): $S_f = 2^{\frac{1}{2}} + 0 + 2^{\frac{1}{2}} + 1 + 2^{\frac{1}{2}} + 1 + 0 + 1 = 3 + 3\ 2^{\frac{1}{2}}$

Final state 3 (Fig. 2d): $S_f = 0 + 1 + 2^{\frac{1}{2}} + 1 + 0 + 1 + 2^{\frac{1}{2}} + 1 = 4 + 2\ 2^{\frac{1}{2}}$

Final state 4 (Fig. 2e): $S_f = 2^{\frac{1}{2}} + 1 + 2^{\frac{1}{2}} + 0 + 2^{\frac{1}{2}} + 0 + 2^{\frac{1}{2}} + 1 = 2 + 4\ 2^{\frac{1}{2}}$

Final state 5: $S_f = 0$

Final state 6 (Fig. 2f): $S_f = 0 + 1 + 2^{\frac{1}{2}} + 0 + 2^{\frac{1}{2}} + 0 + 2^{\frac{1}{2}} + 0 = 1 + 3\ 2^{\frac{1}{2}}$

Final state 7: $S_f = 0$

Final state 8: $S_f = 0$

The possible entropy changes are

$$\Delta S = S_f - S_i = \left\{0, \sqrt{2}, 1, -1 + 2\ 2^{\frac{1}{2}}, -3 - 2\ 2^{\frac{1}{2}}, -2 + 2^{\frac{1}{2}}, -3 - 2\ 2^{\frac{1}{2}}, -3 - 2\ 2^{\frac{1}{2}}\right\}.$$

Temperature and pressure dependences of exchange in the complex pore

Relevant results for the pore structure of Fig. 3a are summarized in six graphs in Fig. S3. All parameters are relative quantities without units. The top three graphs a), b) and c) show the variation of a_{sy} with temperature for a population fraction of 0.2 corresponding that of a gas. The asymmetry parameter assumes positive and negative values in a seemingly erratic but reproducible manner in the range of -0.7% < a_{sy} < 0.4% for repulsive interaction (Fig. S3a), i. e. for the definition of the force between particles as illustrated in Fig. 2a. The interaction can be changed to attractive by changing the sign of ΔU in the expression for the free energy. In this case the asymmetry parameter varies as well, however, only between ≈0% < a_{sy} < 0.5% (Fig. S3b). In either case, up to roughly 0.5% of all jumps on the checkerboard proceed in a circular fashion between the three sites. With reference to Fig. 1, positive a_{sy} reports that the straight entry route from the bulk into the small pore is preferred over the detour via the grain surface. This is the case for attractive interaction at $T < 2$ (Fig. S3b). For repulsive interactions and temperatures $T > 1$, a_{sy} is negative and the opposite route is preferred (Fig. S3a). If the interaction between particles and walls is turned off, i. e. $\Delta A = 0$, then the simulation produces largely noise for a_{sy} (Fig. S3c). The noise level is two orders of magnitude smaller than the maximum absolute values of a_{sy} obtained with either repulsive (Fig. S3a) or attractive interaction (Fig. S3b). This suggests that the non-zero values for a_{sy} reported in Figs. S2a and 4b are trustworthy.

At the extrema of the $a_{sy}(T)$ curves in Figs. S3a,b the dependences of the asymmetry parameters on pressure corresponding to population density were investigated (Figs. S3d-f). The variations with population density are smoother than those with temperature. Positive and negative values of a_{sy} result at a low temperature of $T = 0.2$ for repulsive interaction (Fig. S3d), whereas either negative or positive values arise for repulsive (Fig. S3e) and attractive (Fig. S3f) interactions at higher temperatures of $T = 2.2$ and 1.3, respectively. Interestingly, two well developed positive modes result for attractive interaction at $T = 1.3$.

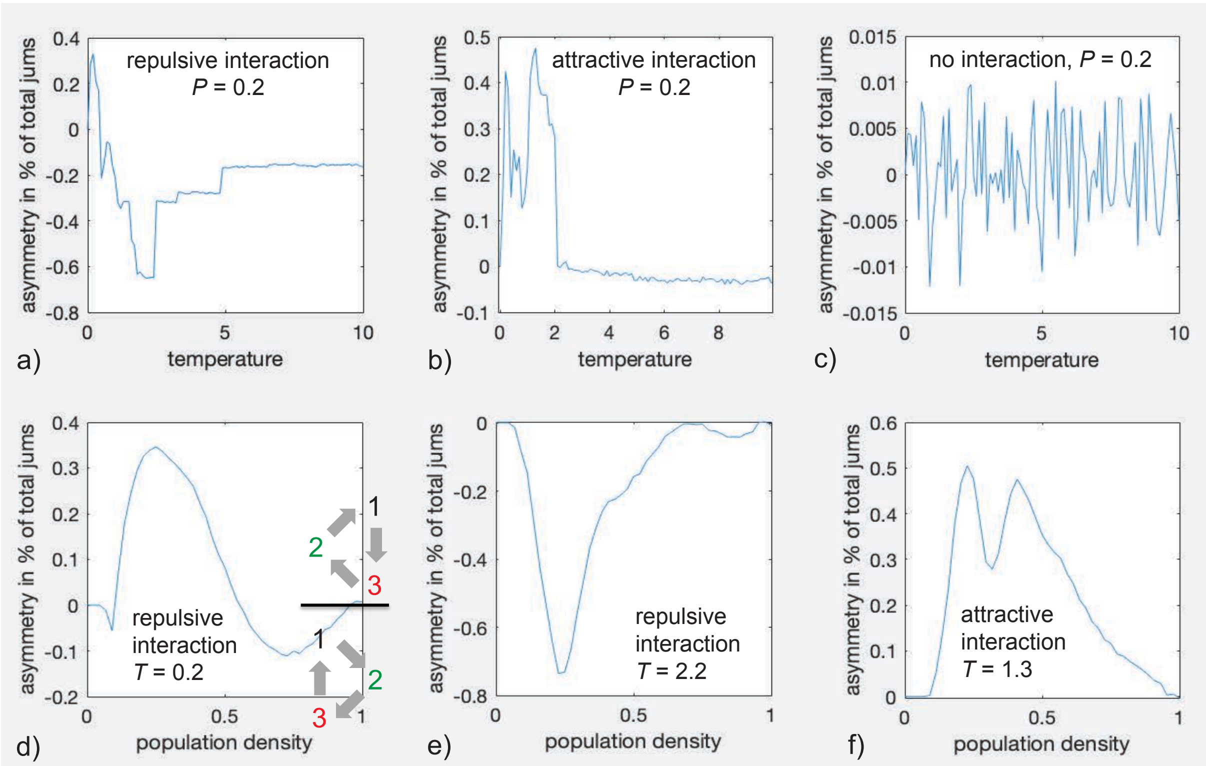

Figure S3. Asymmetry parameters a_{sy} for diffusion in and out of the grain pore depicted in Fig. 3a as a function of relative temperature T (top row) at a population density of 0.2 and relative pressure or population density P (bottom row) at different temperatures. a) $a_{sy}(T)$ for repulsive interaction. b) $a_{sy}(T)$ for attractive interaction. c) $a_{sy}(T)$ without interaction. d) $a_{sy}(P)$ for repulsive interaction at $T = 0.2$. e) $a_{sy}(P)$ for repulsive interaction at $T = 2.2$. f) $a_{sy}(P)$ for attractive interaction at $T = 1.3$.

Population density distributions for different pores and thermodynamic parameters

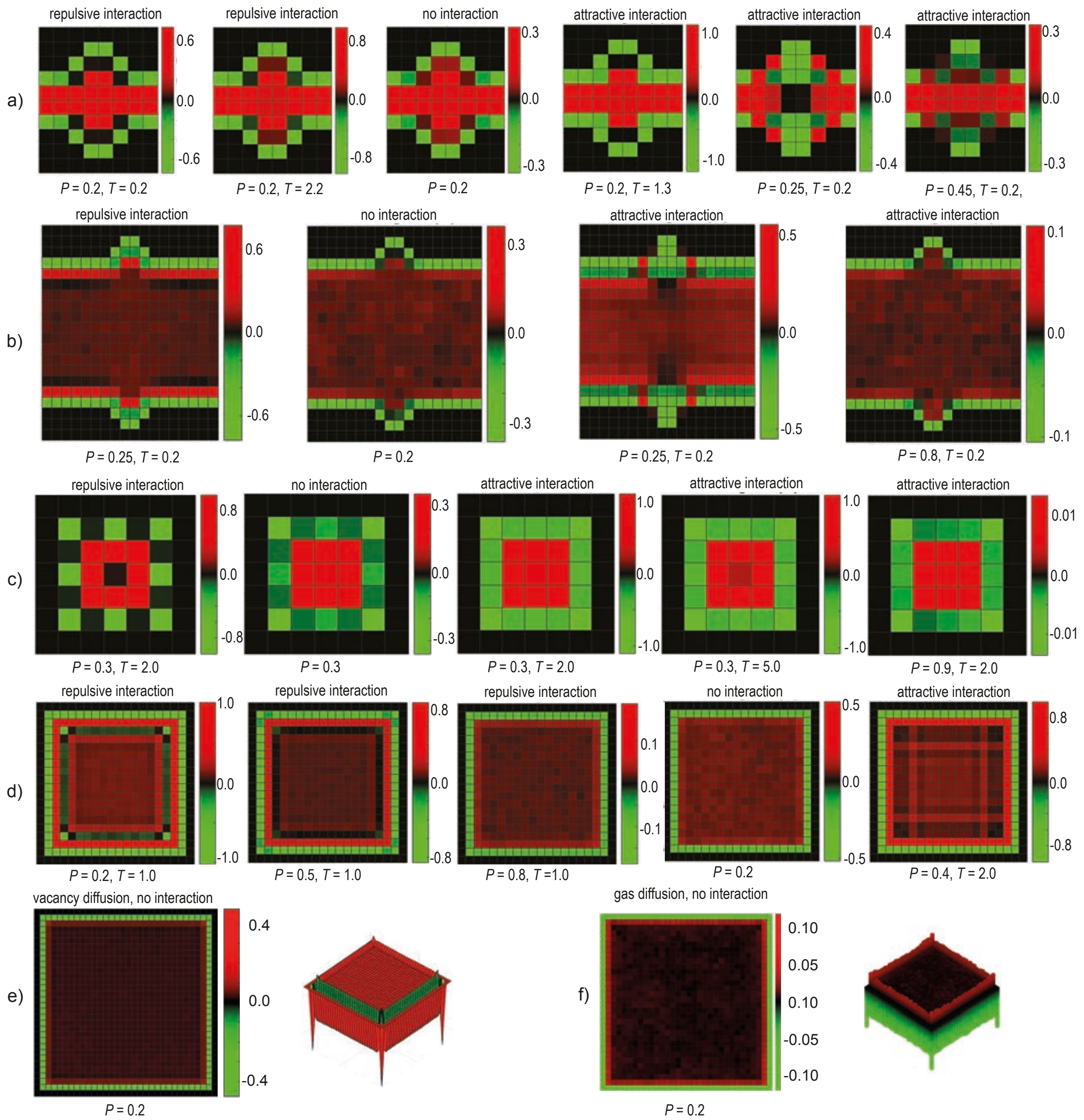

Figure S4. Maps showing the deviations of the particle density from its mean across the pore. a,b) Model for a porous solid, 10^7 jumps. c-e) Square pore, 10^7 jumps. The color scales are different in each plot. The particle concentrations vary more strongly with pressure P than with temperature T. e) Vacancy diffusion in a 32×32 pore with repulsive interaction. f) Gas diffusion in a 32×32 pore without interaction, 10^8 jumps.

Asymmetry parameter for gas diffusion versus exchange time

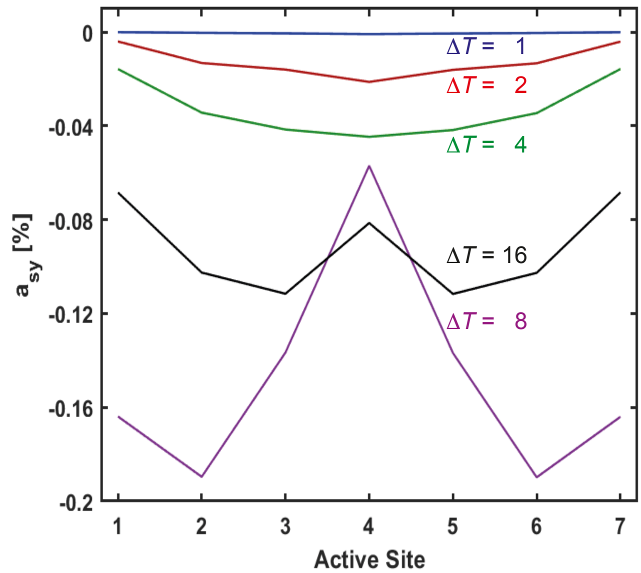

Figure S5. Asymmetry parameters for gas diffusion in the pore of Fig. 6c for different time lags between observations in arbitrary time units (atu). Blue = 1 atu, red = 2 atu, green = 4 atu, purple = 8 atu, black = 16 atu from 5×10^8 steps. The blue curve (1 atu) is the same as the green curve in Fig. 6e.

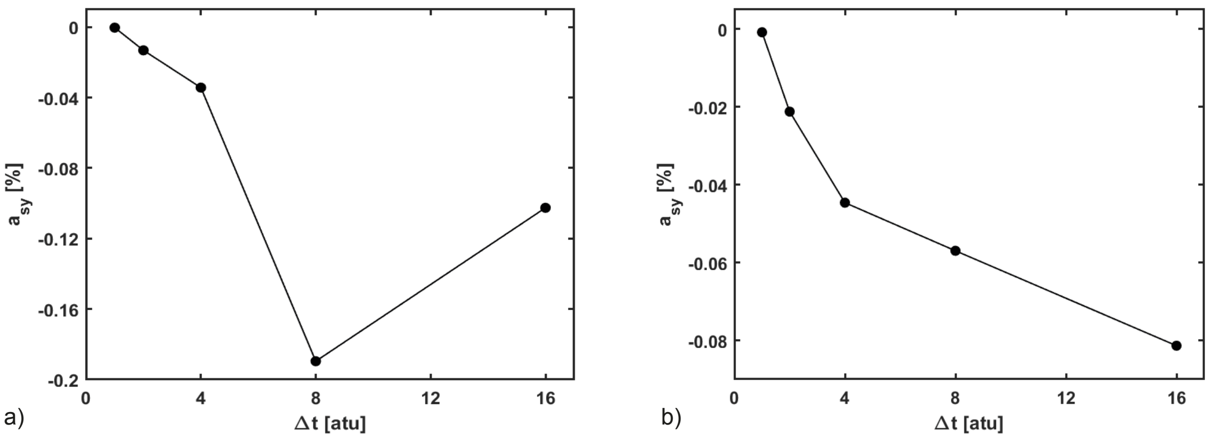

Figure S6. Variation of the asymmetry parameter for gas diffusion in the pore of Fig. 6c at positions 2 (a) and 4 (b) of the active site (cf. Fig. S5) as a function of the time lag Δt in arbitrary time units.